Numerical Approach for the Analysis and Optimization of Phased Array Feed Systems

Marianna Ivashina

The Netherlands Institute for Radio Astronomy (ASTRON)

Supported by part:

- The Netherlands Organization for Scientific Research (NWO);

- VINNOVA (Sweden) – Marie Curie Grant (2010-2012).

Large-field survey with a single-beam telescope

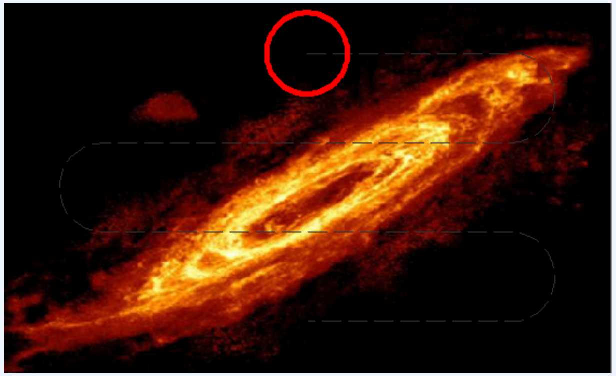

Mosaicing:

-Many observations by mechanically steering the dish, so that the beams closely overlap.

-The large-field image is formed by composing a mosaic of smaller sized overlapping images.

Large-field survey with a single-beam telescope

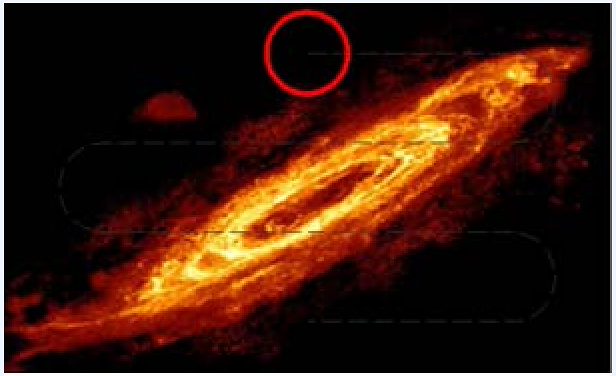

Mosaicing:

-Many observations by mechanically steering the dish, so that the beams closely overlap.

-The large-field image is formed by composing a mosaic of smaller sized overlapping images.

Nyquist's field-sampling theorem:

- Beam separation < 0.5HPBW
  for uniform sensitivity.

- The maximum allowable ripple less ~20%.

Enhancing large-field surveys with PAFs

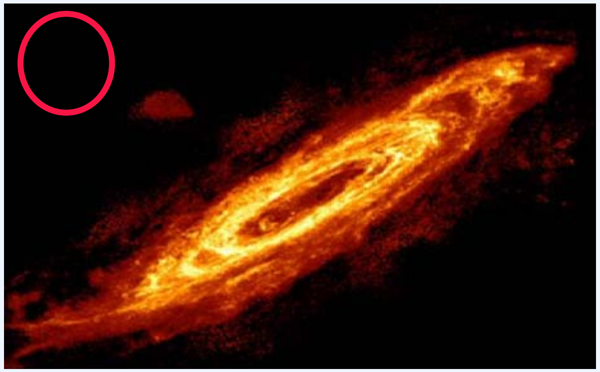

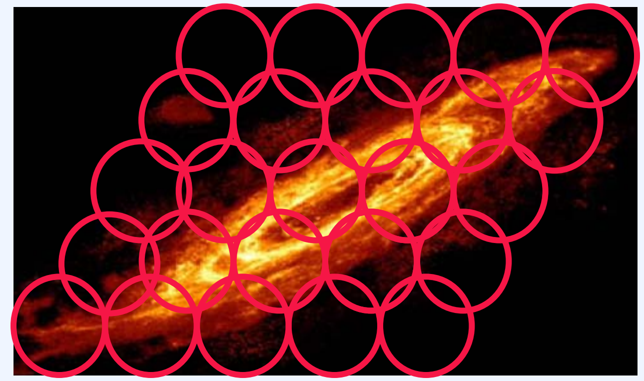

many beams in one snapshot

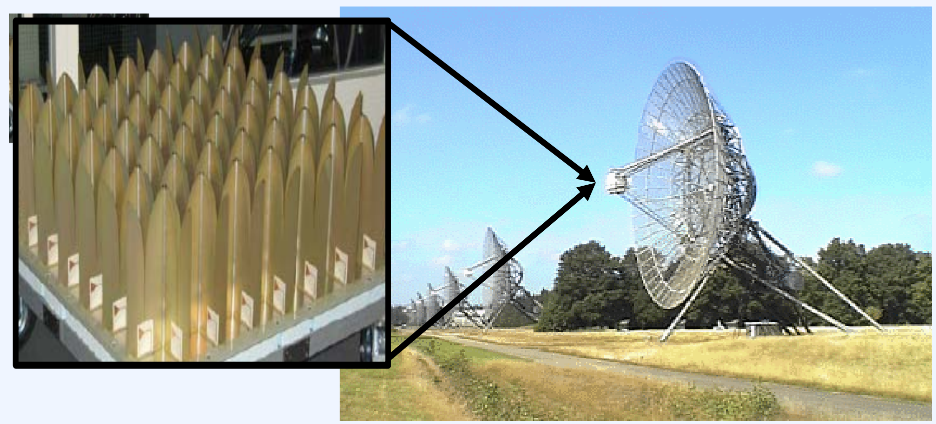

Conventional singe-beam feed

PAFs of electrically small elements

Performance trade-off

- The required field-sampling limit – a cost effective # of beams:

  ⇒ *the maximum sensitivity should be traded against the maximum tolerable ripple over FOV.*

- High polarization purity – sensitivity:

  ⇒ *high beam stability and good intrinsic polarization of the system, in order to reduce the corrections for the instrumental polarization in the beamformer, that may compromise the sensitivity.*

- Wide frequency band

Analysis and optimization of PAF systems

Challenging problem: understanding the interaction between

Antenna element mutual coupling

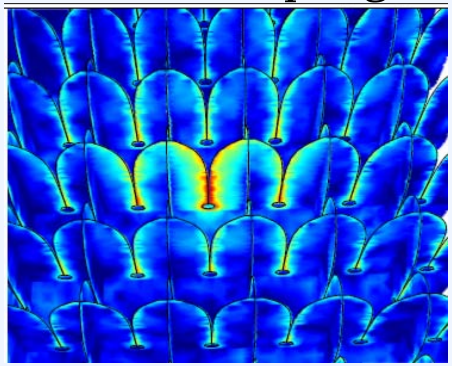

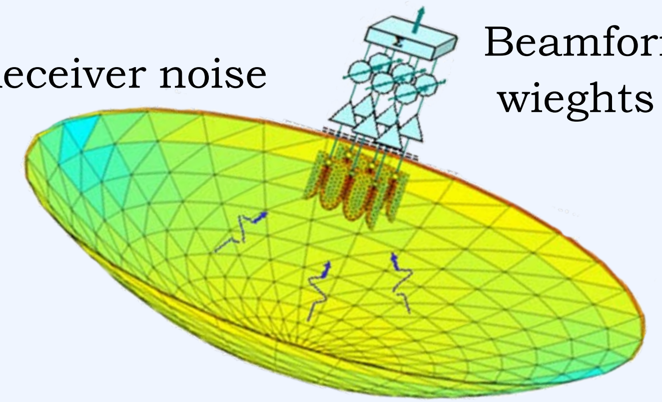

‘ + ’ multiple closely overlapping beams over a wide frequency band;

‘ — ’ strong correlation between signal/noise waves

⇒ A combined antenna-LNA-signal processing problem.

Accurate and computationally efficient numerical methods and tools

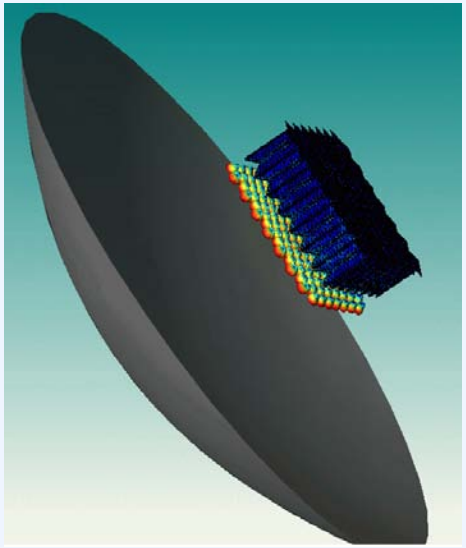

A newly developed numerical toolbox* for CAESAR**:

Interface with GRASP9
to perform a system analysis
and beamformer optimization.

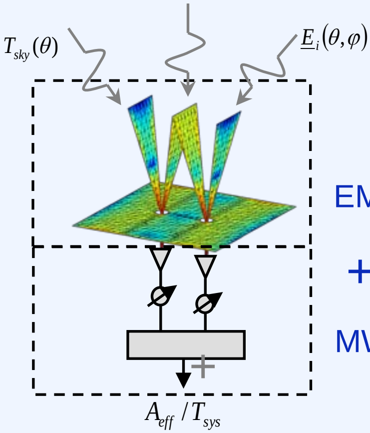

Signal processing algorithms***:

CFM, MaxSNR, LCMV.

Applied to model the DIGESTIF system (144 elements).

NUMERICAL METHODS:

- **M.V. Ivashina, O. Iupikov, W. van Cappellen, ''A New Numerical Toolbox of the CAESAR Software for Analysis and Optimization of Reflector Antennas Phased Array Feed Systems', ICEAA2010, Sydney, Australia, Sept. 20-24, 2010.*
- ***R. Maaskant, "Analysis of large antenna systems," Ph.D. dissertation, Eindhoven Univ. of Technology, The Netherlands, June 2010.*
- ****M. V. Ivashina. O.Iupikov, R.Maaskant, W. van Cappellen, T. Oosterloo, 'An Optimal Beamforming Strategy for Wide-Field Surveys With Phased-Array-Fed Reflector Antennas', re-submitted to IEEE Trans. on AP.*

Details on beamforming scenarios

1. $\mathbf{w}_{\mathrm{CFM}} = \mathbf{e}.$

2. $\mathbf{w}_{\mathrm{MaxSNR}} = \mathbf{C}^{-1}\mathbf{e}, \quad \text{with} \quad \mathrm{SNR} = \mathbf{w}^{H}_{\mathrm{MaxSNR}}\mathbf{C}^{-1}\mathbf{w}_{\mathrm{MaxSNR}}$

   Does not guarantee smooth variation within the BW.

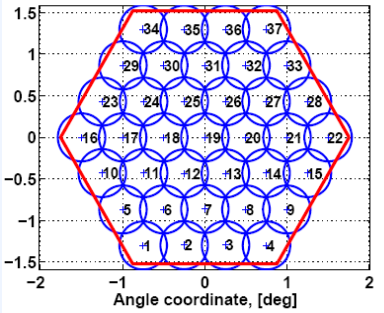

Arrangement and numbering of the beams on the sky

3. More uniform sensitivity by broadening each beam (by imposing additional constraints on the cross-over points between adjacent beams). $\Rightarrow$

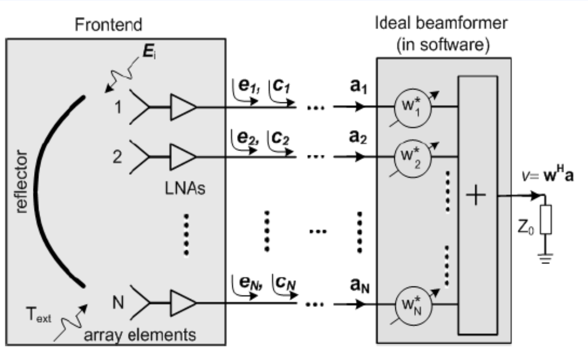

$$\mathbf{w}^{H}_{\mathrm{MaxSNR\&Constr}} = \mathbf{g}^{H}\left[\mathbf{G}^{H}\mathbf{C}^{-1}\mathbf{G}\right]^{-1}\mathbf{G}^{H}\mathbf{C}^{-1}$$

$$\mathbf{G} = \left[\mathbf{e}(\Omega_1) \;\vdots\; \mathbf{e}(\Omega_2) \;\vdots\; \cdots \;\vdots\; \mathbf{e}(\Omega_{N_{\mathrm{dir}}})\right]$$

$$\mathbf{g} = [g_1, \quad g_2, \quad \cdots, \quad g_{N_{\mathrm{dir}}}]^T$$

determined in an iterative process, such that the sensitivity loss at the beam center is at most 10% with respect to the sensitivity without constraints.

Apertif Prototype System

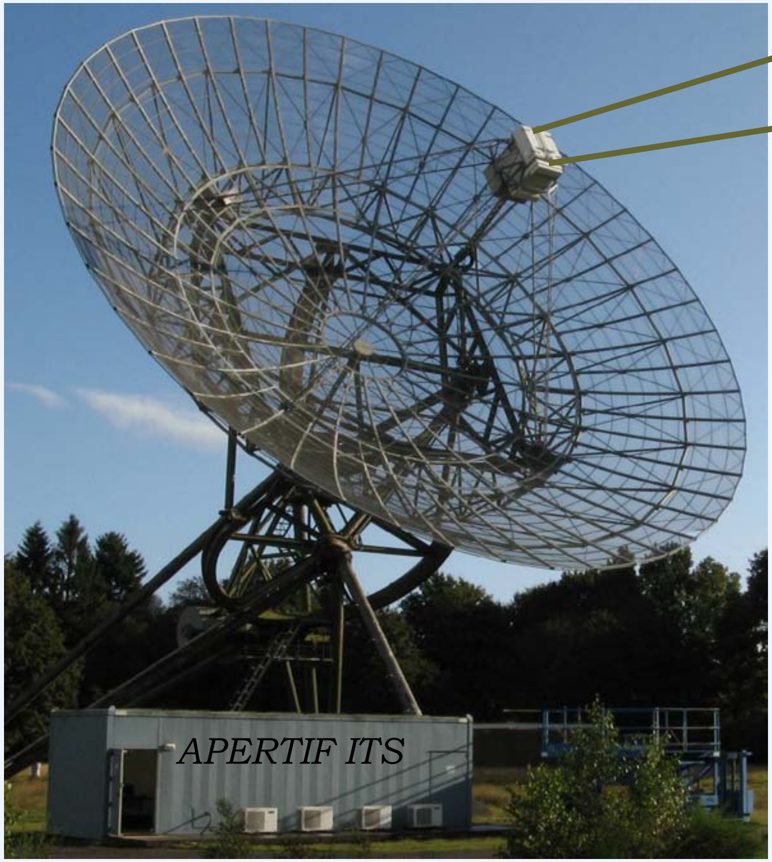

System Prototype:

- Dual-polarized FPA (*1 GHz – 1.75 GHz).*
  - *144 TSA elements (10cm=0.5λ@1.4GHz);*
  - *1mx1m feed box.*
- 56 active receiver channels (1 pol.)

Experimental Platform:

- 1 of WSRT reflectors (25m);
- Digital data recording-storing facilities;
- Beamforming (off-line);
- Opt. algorithm for max beam sensitivity.

Antenna array model

- is based on combining an EM model of the dielectric-free antenna array (CBFM) with a MW circuit model of the TSA microstrip feed.

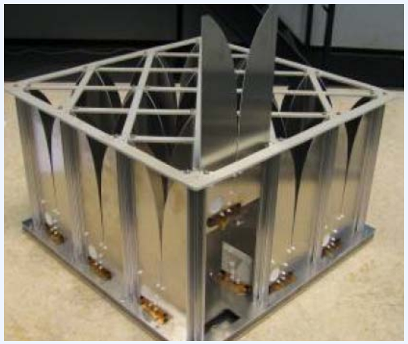

=

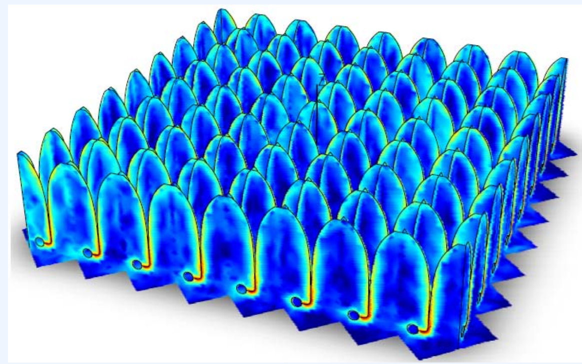

+

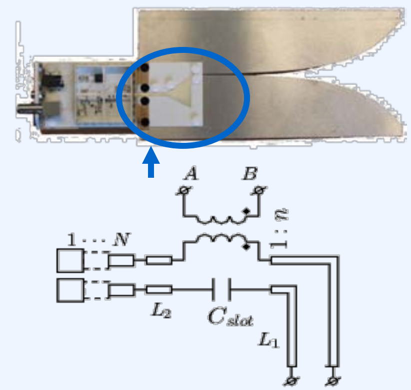

- significantly reduce the computational burden.
- demonstrates a good agreement between measurements and simulations (max. relative difference is 20%).

See details of this approach in R. Maaskant, M. V. Ivashina, O. Iupikov, E. A. Redkina, S. Kasturi, and D. H. Schaubert, Analysis of Large Microstrip-Fed Tapered Slot Antenna Arrays by Combining Electrodynamic and Quasi-Static Field Models, to appear in 2010 in IEEE Trans. on AP.

Active reflection coefficients of array elements for 37 beam directions

CFM

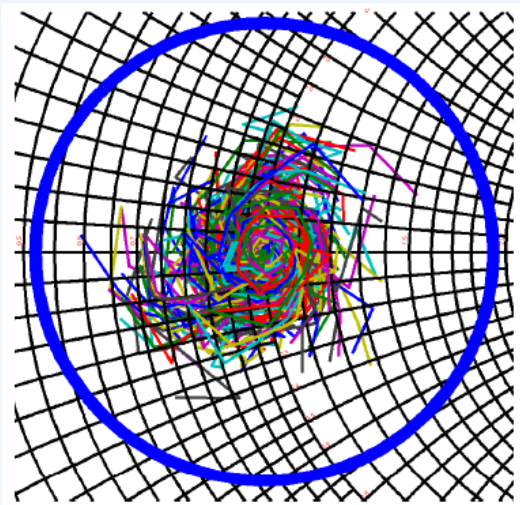

[illegible]	-18.2	-20.1	-17.7	-18.4	-21.5	-19.0	[illegible]
-17.7	-17.0	-16.2	-15.2	-16.1	-16.4	-17.1	-17.1
-19.1	-16.3	-10.9	-12.3	-12.5	-10.8	-16.0	-18.7
-12.8	-10.1	-8.3	-5.8	-5.7	-8.5	-10.1	-12.9
-11.8	-8.4	-3.8	-0.0	-0.0	-3.7	-8.4	-12.1
-12.6	-10.3	-8.5	-5.8	-5.8	-8.3	-10.0	-12.6
-18.5	-16.1	-10.5	-12.0	-12.5	-10.9	-16.4	-18.8
-17.7	-17.2	-17.0	-15.6	-15.3	-16.4	-17.4	-17.9
[illegible]	-18.6	-22.1	-17.8	-17.7	-20.7	-18.4	[illegible]

MaxSNR

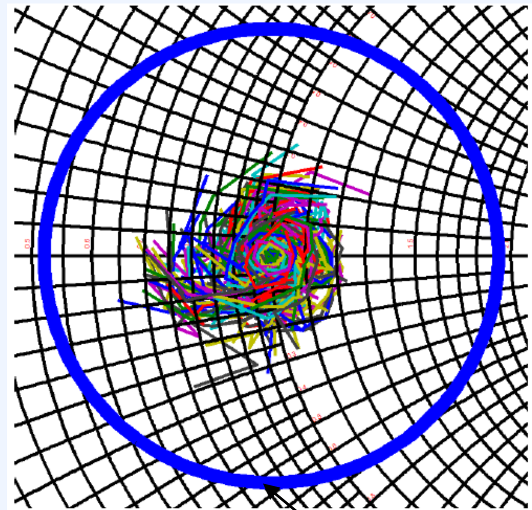

-10dB

MaxSNR&Constr

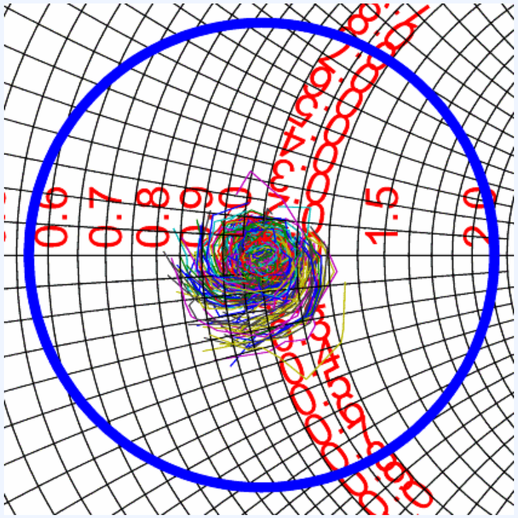

[illegible]	[illegible]	-24.9	-25.4	-25.4	-25.1	[illegible]	[illegible]
[illegible]	-25.7	-20.7	-21.5	-21.7	-21.5	[illegible]	[illegible]
-24.1	-20.2	-19.0	-14.9	-14.8	-19.2	-20.6	-24.5
-20.8	-18.1	-10.9	-7.0	-7.0	-10.7	-17.5	-20.3
-18.3	-15.5	-8.5	-0.1	-0.0	-8.4	-15.8	-18.5
-20.5	-17.6	-10.6	-7.0	-7.0	-10.8	-17.7	-20.2
-24.7	-20.3	-19.1	-14.8	-15.2	-18.7	-20.1	-23.5
-25.6	-27.1	-22.2	-21.0	-21.8	-21.6	[illegible]	[illegible]
[illegible]	[illegible]	-25.0	-25.3	-25.7	-24.6	[illegible]	[illegible]

System noise temperature

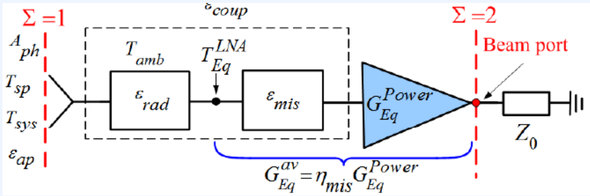

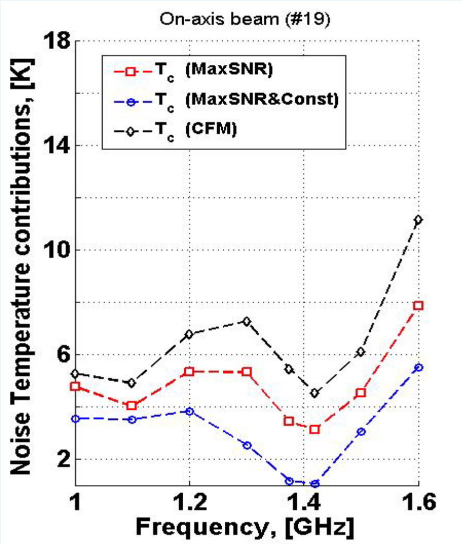

Noise coupling

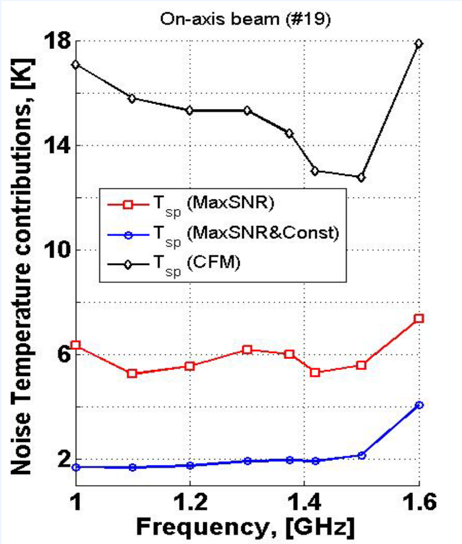

Spillover loss

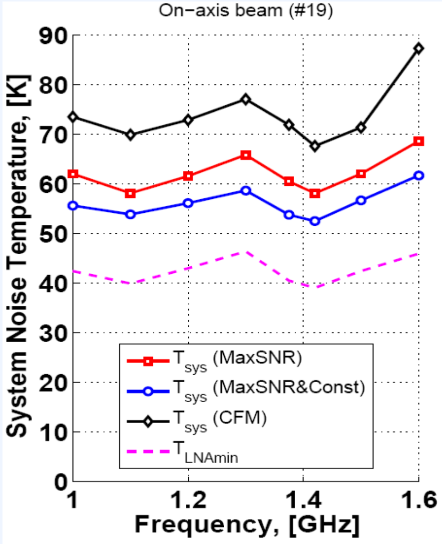

Total T_{sys}

$$T_{out}^{LNA} = \sum_{m=1}^{M} G_m^{av} T_m^{LNA}$$

$$T_m^{LNA} = T_{min} + \frac{4R_n T_o}{Z_o} \frac{|\Gamma_{act,m} - \Gamma_{opt}|^2}{|1+\Gamma_{opt}|^2(1-|\Gamma_{act,m}|^2)}$$

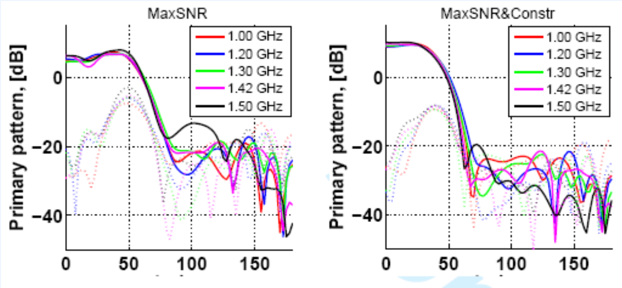

(b) $\phi = 45°$

Antenna ohmic losses

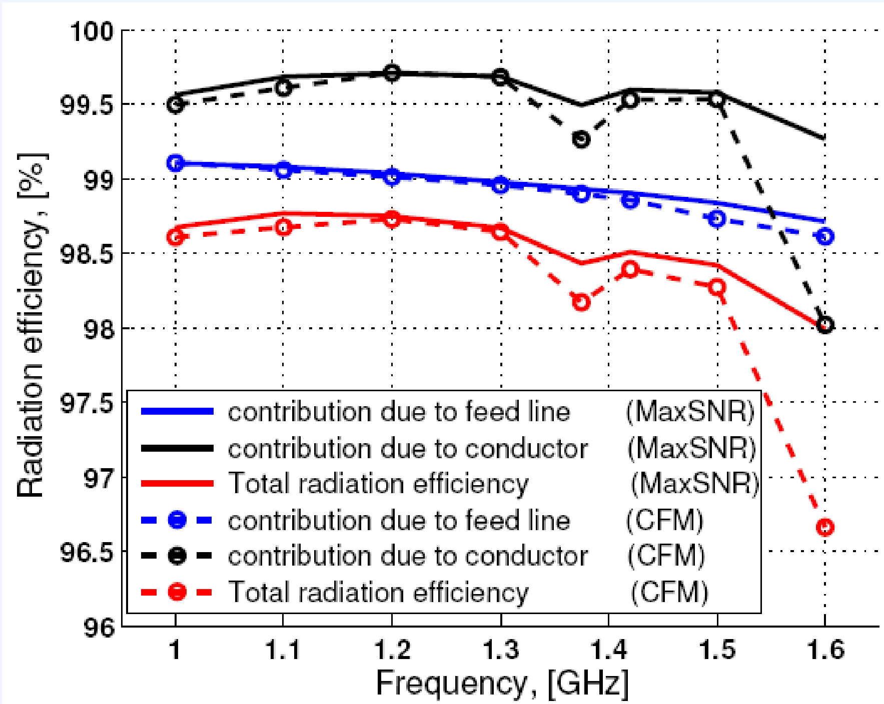

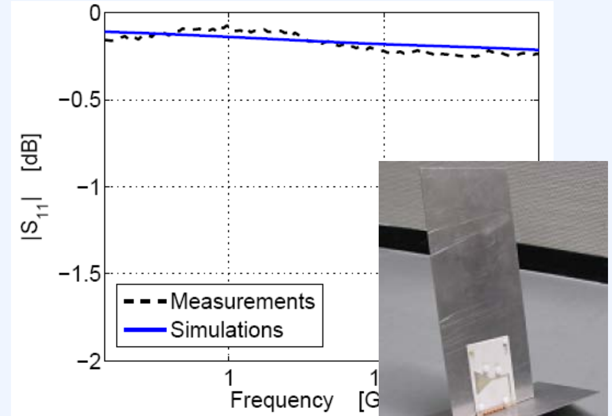

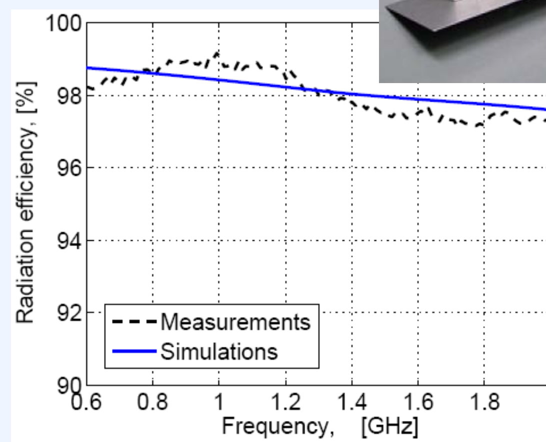

$T_{\mathrm{ant}} = T_{\mathrm{amb}}(1-\eta_{\mathrm{rad}})/\eta_{\mathrm{rad}}$ 4 K - 5 K at $T_{\mathrm{amb}} = 300$ K.

Maaskant, R. Bekers, D.J., Arts, M.J., van Cappellen, W.A., Ivashina, M.V., 'Evaluation of the Radiation Efficiency and the Noise Temperature of Low-Loss Antennas,' *Antennas and Wireless Propagation Letters, IEEE*, Dec. 2009, vol. 8, p. 1166-1170.

Beam patterns and aperture efficiency

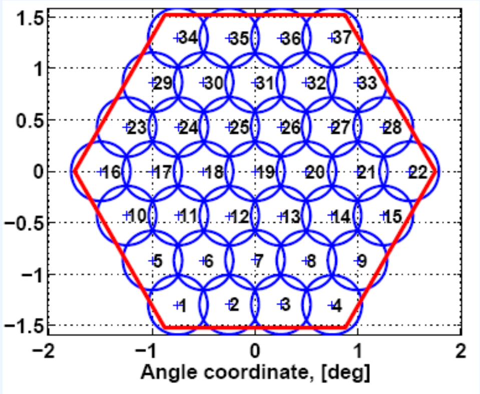

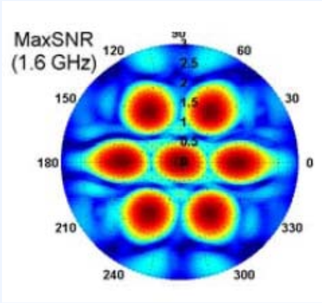

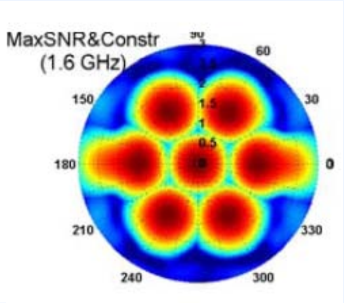

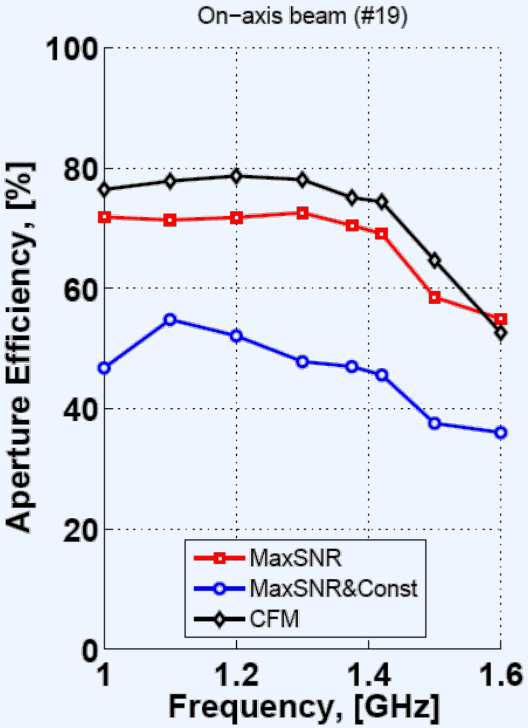

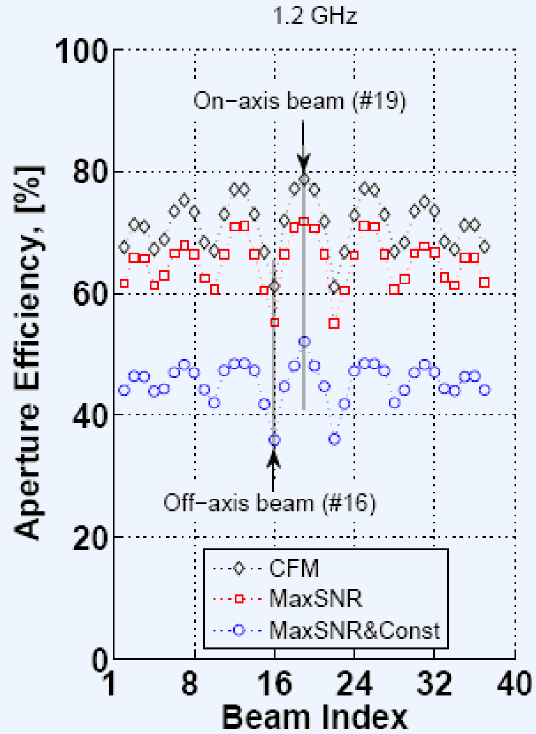

Beams # 19 (on-axis), 17, 30, 32, 21, 8, 6.

Normalized sensitivity maps

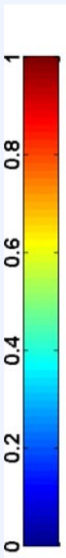

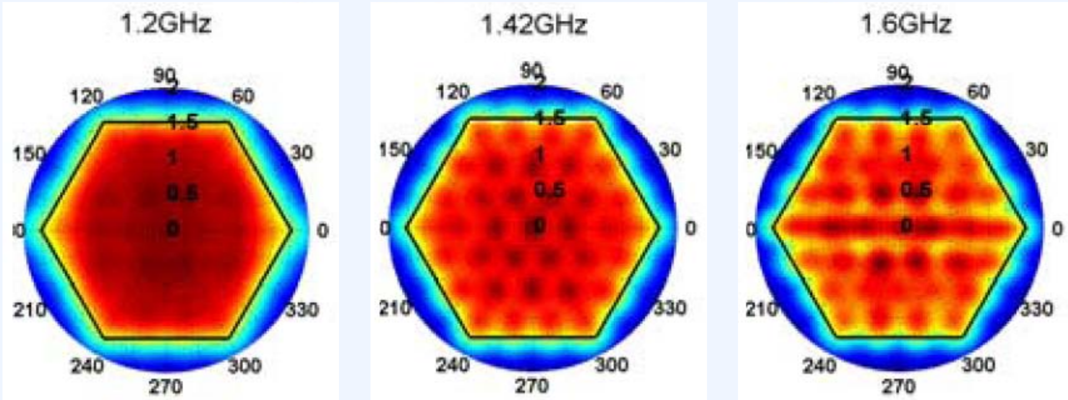

1 dish pointing (MaxSNR)

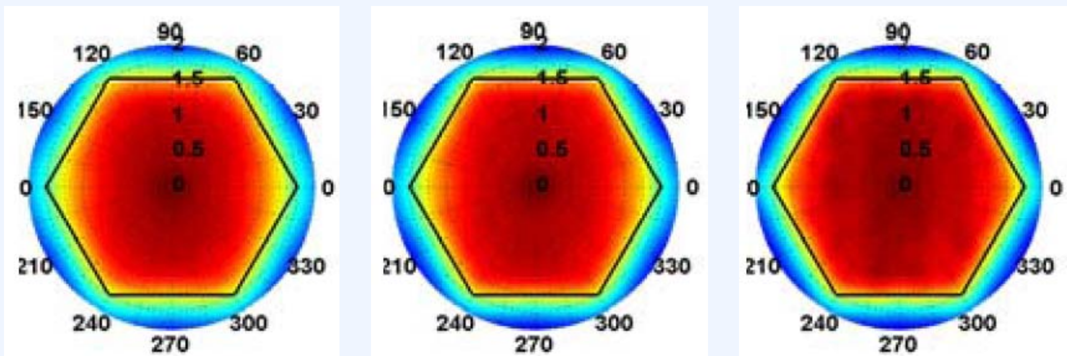

1 dish pointing (MaxSNR&Constr)

7 dish pointings

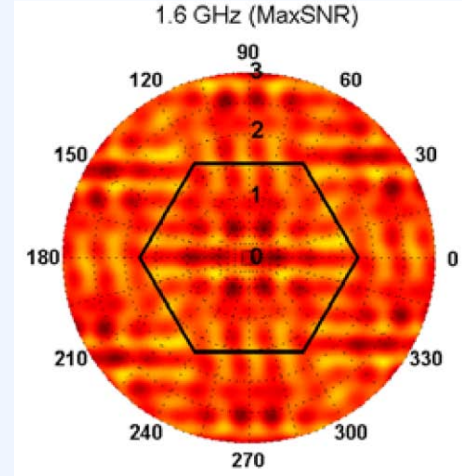

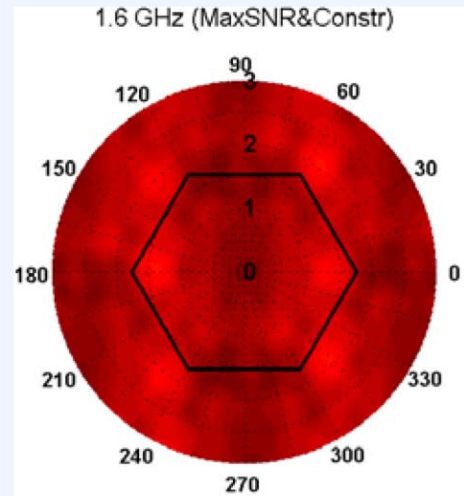

Maximal sensitivity ripple vs. frequency

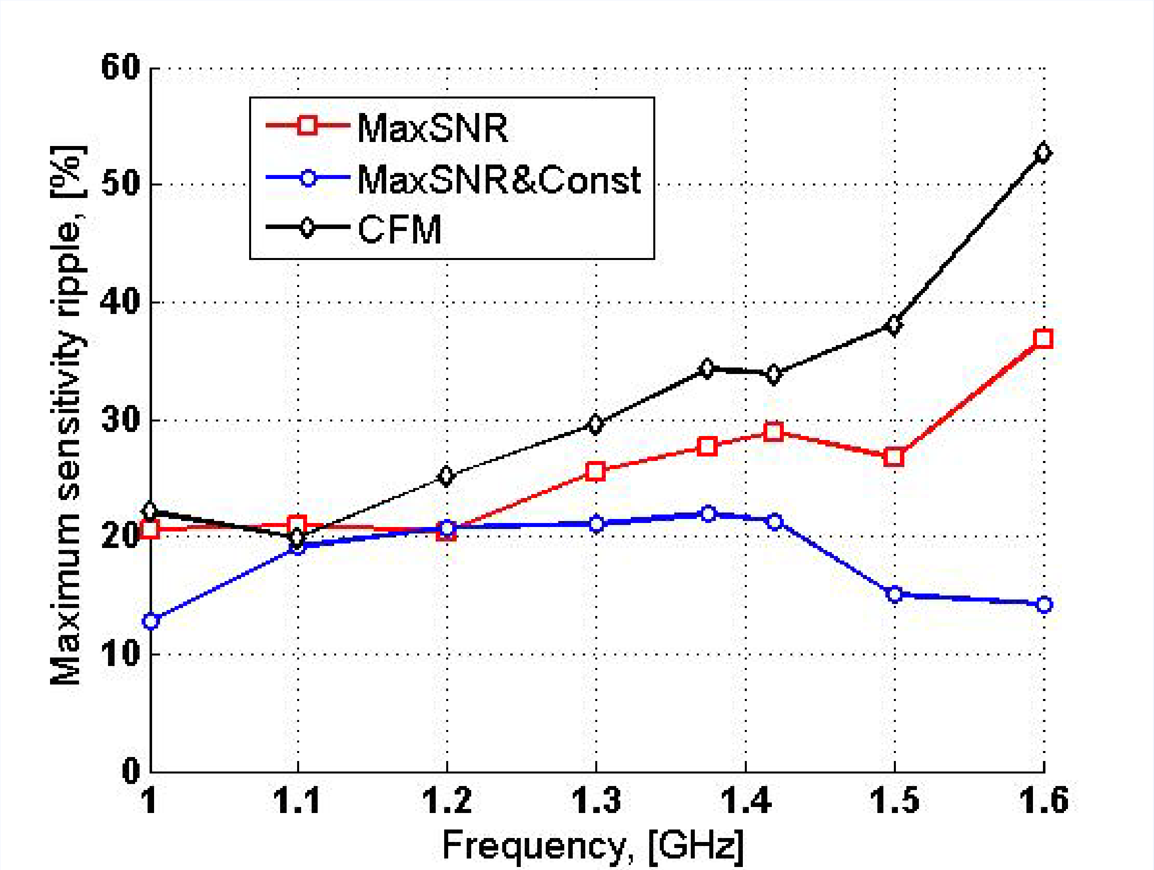

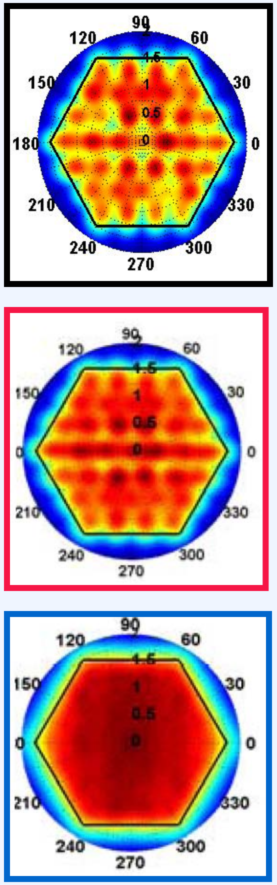

1.6 GHz

Maximal sensitivity ripple vs. # beams

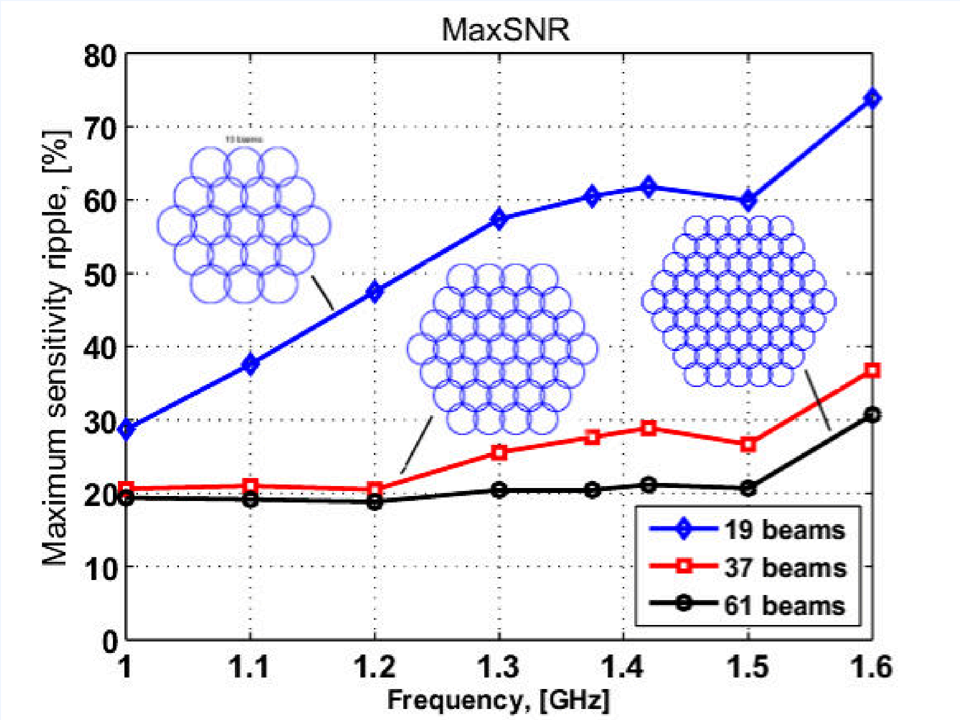

MaxSNR beamformer would require almost twice as many beams to cover the same area of the FOV with a max ripple of 20%.

Simulated and Measured Beam Sensitivities

Each beam is optimized for MaxSNR

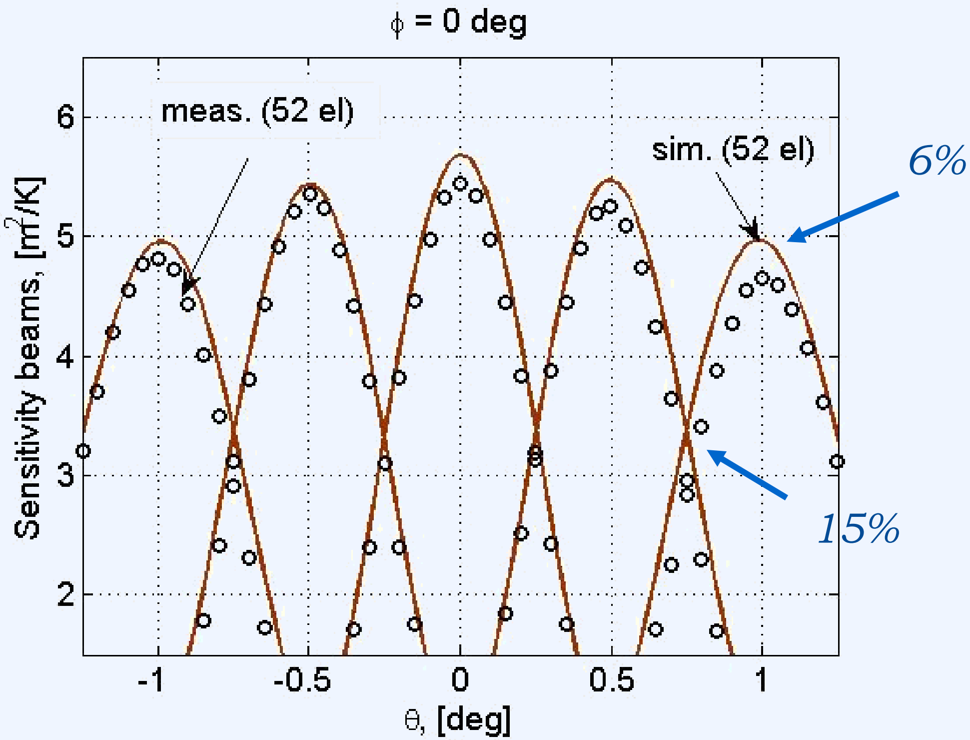

Simulated and measured sensitivities for the 52-channel beamformer

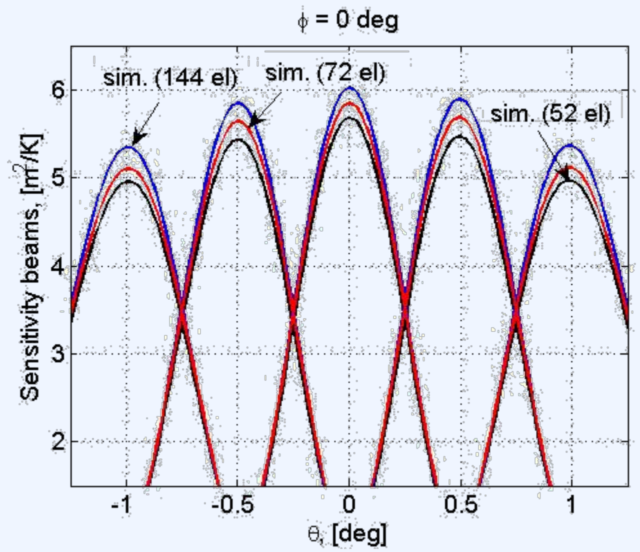

Simulations for beamformers with 52, 72 and 144 channels

Simulated and Measured Sensitivity over FOV

Each of the 31x31 beams is optimized for MaxSNR

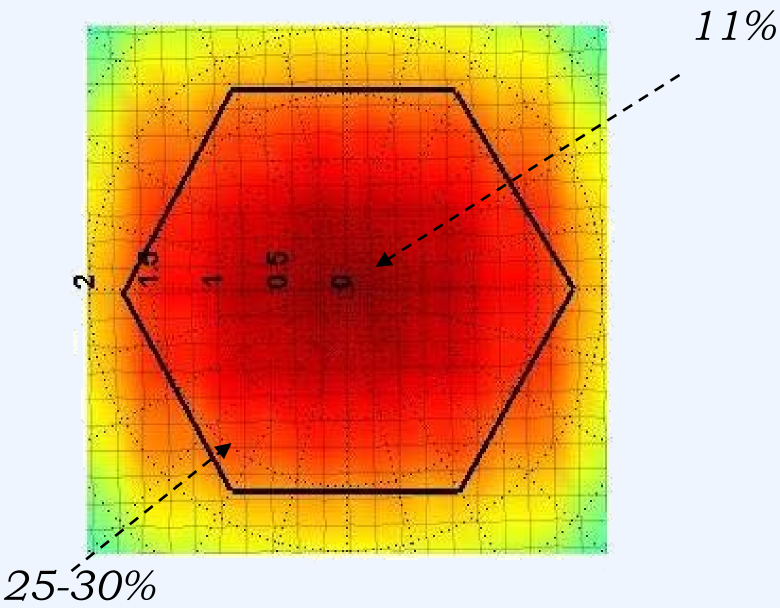

Increased relative difference is due to reduced model accuracy for the edge elements (absence of the feed box and struts)

Simulations

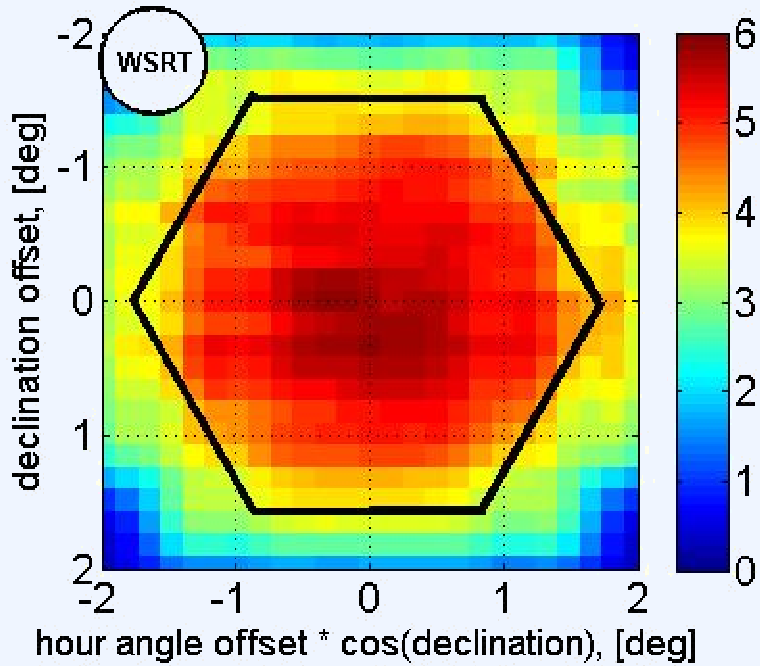

Measurements

Simulated Polarization Discrimination over FOV

IXR is a measure of the orthogonally between the beam channels and differential gain difference [T. Carrozi].

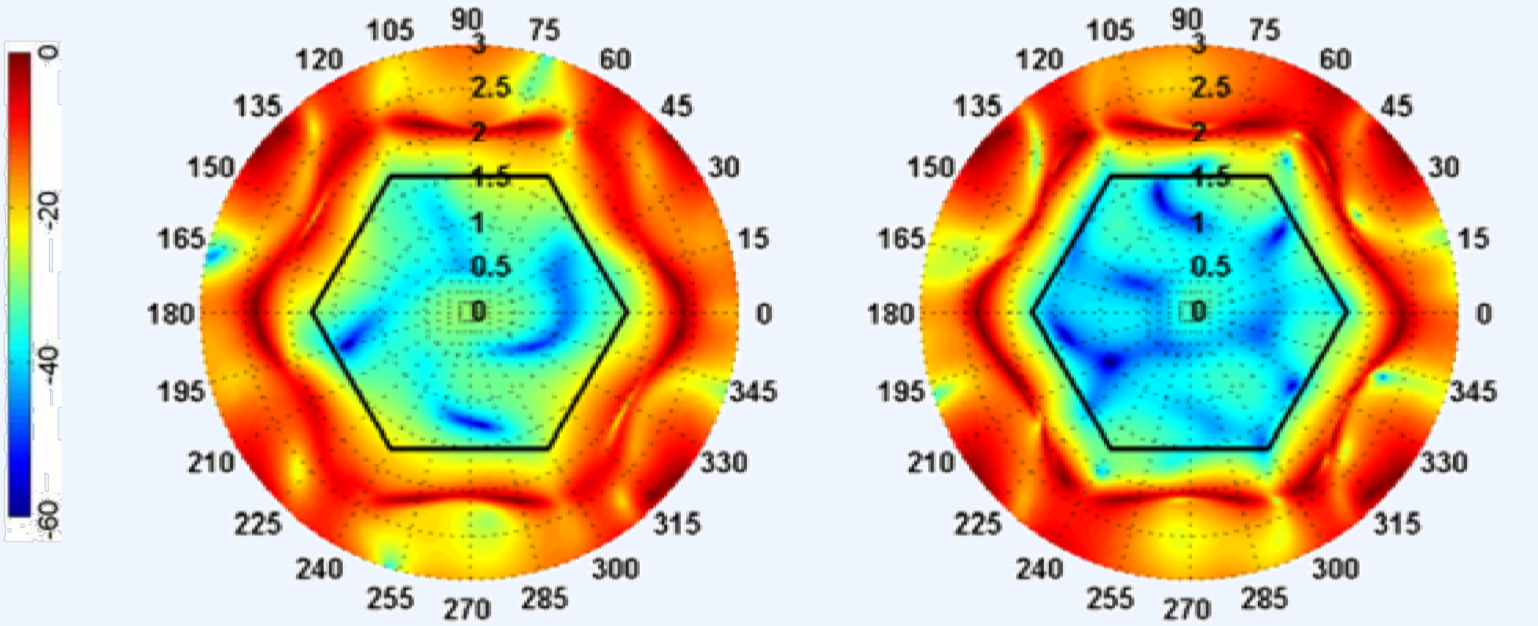

Bi-scalar SNR beamformer (equally oriented elements)

Full-polarization SNR beamformer (equally oriented elements)

Note: the models does not account for the effects of struts.

Polarization discrimination vs. frequency

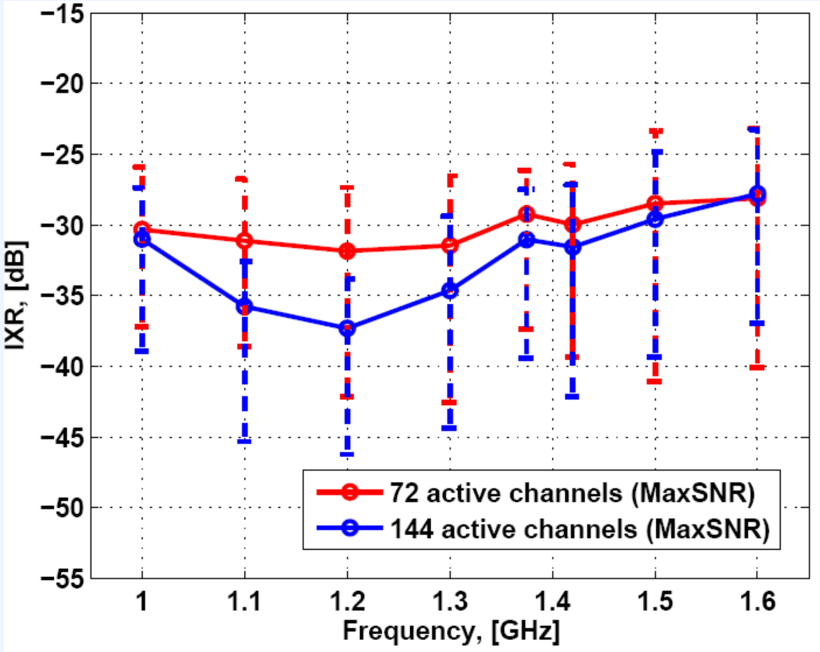

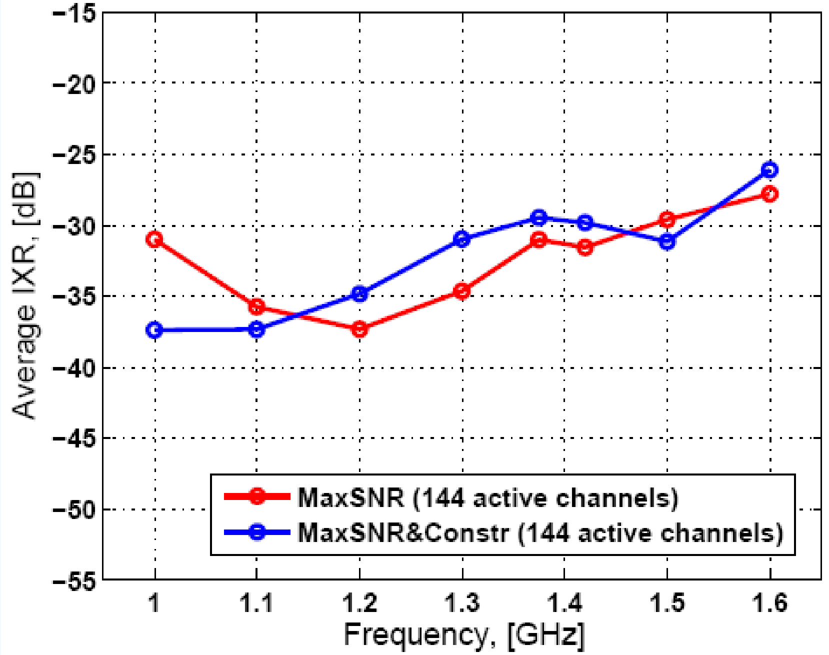

Effects of struts on polarization (initial results)

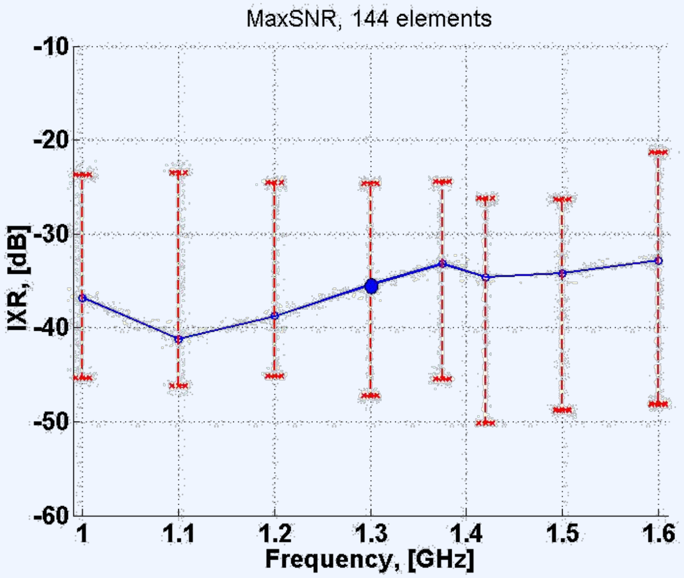

1.3 GHz (no struts)

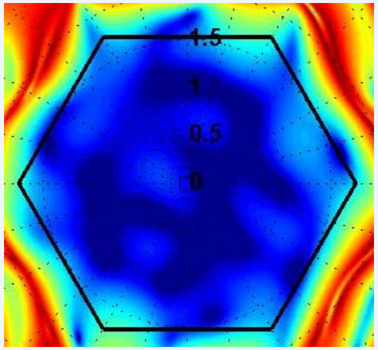

$(IXR)_{av}$ = -36 dB

1.3 GHz (struts)

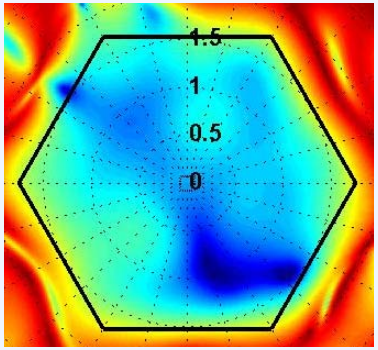

$(IXR)_{av}$ = -25 dB

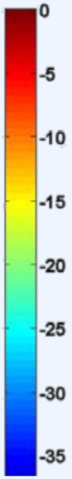

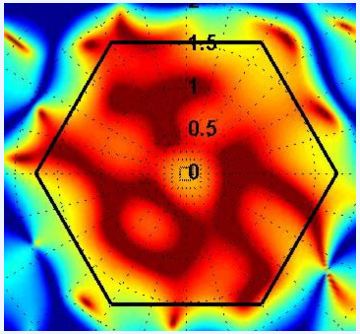

$(XPD)_{co}$ = 43 dB

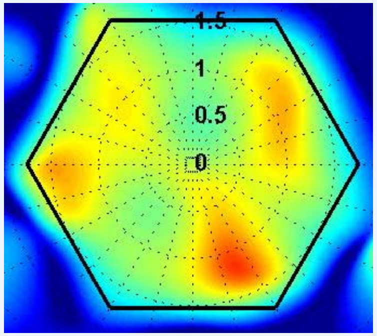

$(XPD)_{co}$ = 23 dB

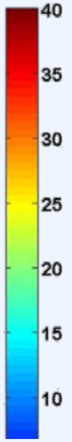

Initial modeling results on the beam stability and polarization variation

1. The shape of a non-calibrated compound beam is stable within ±2% at the HPBW level (when the phase drifts < 6deg).

2. The impact of the phase drifts of the receiver gains is more severe than that of amplitude drifts.

3. For interferometer, this corresponds to ±1% visibility variation.

$$V(u,v,w) \approx V(u,v,0) = \int_{-\infty}^{\infty}\int_{-\infty}^{\infty} \frac{A_N(l,m)I(l,m)}{\sqrt{1^2 - l^2 - m^2}} e^{-j2\pi(ul+vm)} \mathrm{d}l\mathrm{d}m$$

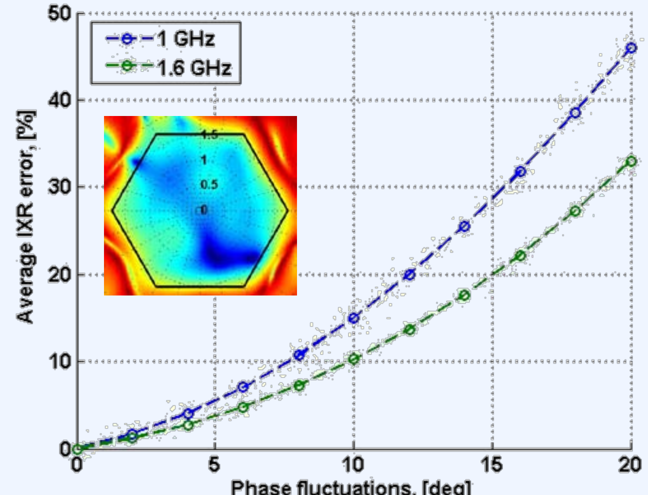

4. A relative variation of the instrumental polarization during observations can be large (10% of IXR@25dB).

Conclusions

The use of a linear constrained minimum variance (LCMV) beamformer was demonstrated to shape the PAF beams

The beam patterns can be broadened, and the sensitivity ripple be reduced to 12 – 22% over the entire bandwidth (while compromising the peak sensitivity no more than 10% with respect to the MaxSNR scheme

The polarization purity has been characterized. It is deteriorated due to field scattering from struts (15dB for non-calibrated beams)

A small sensitivity improvement of about 3 – 4% is observed when all elements are used to form a beam (good intrinsic polarization characteristics of the array).

Conclusions on model verification

The simulated and measured sensitivities are in very good agreement

The worst case relative difference (at the edge of the field of view) is about 30%

This is a satisfactory result, since the system model neither accounts for reflector feed interactions nor for the actual array environment inside the feed box